J. KOSAE Vol. 20, No. E2(2004) pp. 43~52
Journal of Korean Society for Atmospheric Environment

Evaluation of Methyl Iodide (CH_3I) Flux Based on Airborne Field Observations

Zang-Ho Shon
Department of Environmental Engineering, Dong-Eui University, Busan, Korea

(Received 30 January 2004, accepted 8 March 2004)

Abstract

A total of 10 boundary layer sampling events over the Pacific Ocean were analyzed for the purpose of defining the sea-to-air CH_3I flux using a mass balance photochemical model. These events were recorded on the National Center for Atmospheric Research (NCAR) *C-130* aircraft as part of the Aerosol Characterization Experiment (ACE 1). The latitude range, covered by these events, was 2° N to 55° S. The flux ranges were 4 to 33 nmol m^{-2} day^{-1}, with an average value of 11 ± 8 nmol m^{-2} day^{-1}. This study also indicated that the current approach to estimate the flux was not systematically different from the sea-air exchange model.

Key words : Marine flux, Methyl iodide, Air-sea exchange, Pacific ocean, ACE 1

1. INTRODUCTION

It has been reported that methyl iodide (CH_3I) in seawater is produced by microalga (Itoh *et al.*, 1997) and macroalga (Manley and Dastoor, 1988). Oceanic emission of methyl iodide has been known to be a primary source of natural atmospheric CH_3I in the remote marine troposphere (Singh *et al.*, 1983; Lovelock *et al.*, 1973). Some other natural monohalomethane compounds (CH_3Br and CH_3Cl) are also found in the troposphere. Compared with other monohalomethanes, CH_3I is a photochemically reactive species in the tropospheric chemistry. The photolysis of CH_3I by solar radiation that penetrates to the troposphere produces iodine atom (I), which can participate in the tropospheric chemistry. Davis *et al.* (1996) drew attention to its potential role in ozone loss in the troposphere as well as in the stratosphere. Some recent field and modeling studies indicated the significance of the direct, iodine-catalyzed destruction of ozone in the marine boundary layer (MBL) (Shon and Kim, 2002 and reference therein). In addition, iodine chemistry might have an influence on HO_x (= $OH + HO_2$) and NO_x (= $NO + NO_2$) chemistry through converting HO_2 to OH and NO to NO_2. Since the major source of atmospheric iodine is certainly the emission of biogenic iodocarbons from the open ocean or coastal regions, the estimation of the CH_3I emission rate is important for the investigation of its impact on atmospheric iodine chemistry.

The methods used to estimate the fluxes of trace gas species from the ocean to the atmosphere have fallen into two categories: those based on seawater measurements (Wanninkhof, 1992; Liss and Merlivat, 1986) and those inferred from atmospheric observations (Shon, 1999 and references therein). A

---

* Corresponding author.
E-mail : zangho@deu.ac.kr, Tel : +82-(0)51-890-2078

typical method used to estimate CH_3I fluxes was an air-sea exchange model involving seawater CH_3I measurements. The air-sea exchange model by Liss and Slater (1974) is given by the equation (1) :

$$F_{air-sea} = V_p\left[C_{sw} - \frac{C_{air}}{H}\right] \qquad (1)$$

where $F_{air-sea}$ defines oceanic CH_3I flux; V_p is the exchange coefficient (or piston velocity); C_{sw} and C_{air} represent the CH_3I concentrations in seawater and air, respectively; and H is the Henry's law constant. Once evaluated for a specific set of meteorological conditions, a more general form of the "piston velocity" can be developed via a parameterization equation that takes into account the dependence of the flux on wind speed. Currently, at least three different versions of wind speed parameterization have been employed (Wanninkhof, 1992; Liss and Merlivat, 1986; Smethie *et al.*, 1985). The results from these different approaches have revealed some significant differences in the exchange coefficient, leading to uncertainty for seawater derived fluxes that are as large as a factor of 2 (Andreae, 1986). Thus, in this paper we present an analysis of CH_3I flux estimates with the proposed approach using airborne CH_3I data recorded during the ACE 1 field study. In addition, we present the comparison of our fluxes derived from airborne CH_3I measurements with those derived from shipboard measurements by Moore and Groszko (1999) during the ACE 1 campaign.

2. OBSERVATIONAL DATA

Observational data sets used in this study are ones recorded during the First Phase of the Aerosol Characterization Experiment (ACE 1) field campaign. The ACE 1 campaign was carried out during the months of Nov. and Dec. in 1995. Of the 31 marine flights flown during the ACE 1, eighteen of these (Flights 11-28) were made over the Southern Ocean between Nov. 17 and Dec. 12, 1995. These intensive flights covered the latitude range of 40° S to 55° S and the longitude range of 135° E to 160° E, as shown in Fig. 1. A commonly employed sampling strategy for the National Center for Atmospheric Research's (NCAR) *C-130* aircraft consisted of flying sequential circles at 3 or 4 constant altitudes while moving with the wind field. Sampling on each mission included both boundary layer (BL) and buffer layer (BuL, a mixing zone for the BL and lower

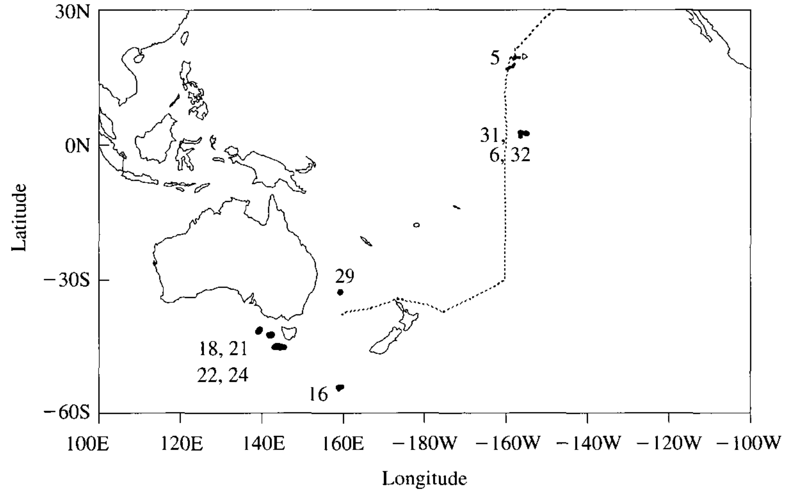

Fig. 1. Marine boundary layer flight tracks for the *C-130* and cruise tracks for the NOAA ship Discoverer during the ACE 1. The number next to each flight track is the field program mission number. The dotted line represents the cruise tracks.

free tropospheric air) altitudes.

This field program included measurements of key chemical species for this study, methyl iodide as well as other nonmethane hydrocarbons. Other critical trace gases measured on the *C-130* included: OH, O_3, CO, CH_4, NO, H_2O_2, and CH_3OOH. All basic meteorological parameters were also recorded during each flight, including the UV irradiance measured by an Eppley radiometer. Methyl iodide as well as other halocarbon measurements on the *C-130* were made using a GC/MS technique (Blake *et al.*, 1999). CH_3I measurements had limit of detection of 0.02 pptv and 1σ measurement precision was 5%. Median concentrations of the photochemical species NO, CO, H_2O, O_3, H_2O_2, CH_3OOH, and CH_4 formed the basis of all input variables to the photochemical box modeling runs (see Table 1) in which the diel profiles for OH were evaluated. In the case of NO, most of the BL observations were at or below the 2σ detection limit of the onboard chemiluminescence NO sensor (e.g., typically 5-10 pptv). Thus, input to the model for NO involved bracketing possible values for NO as defined by our assigning a lower limit value to the measurement of 1 pptv and an upper limit value defined by the 2σ uncertainty for NO. This approach provided upper and lower limit values for OH. The CH_3I flux for these cases was estimated from the OH profile based on the average NO value as defined by the two values cited above. Typically, the level of agreement between observed OH and model generated values for average NO is less than 15%.

During the entire ACE 1 program, the *C-130* aircraft sampled the 118 BL runs. Of these, 47 sampling events were found to be acceptable for estimating CH_3I fluxes. Seventy-one BL runs were excluded from the current analysis because of a lack of airborne CH_3I measurements and large uncertainties in predicting the photolysis rate coefficients and equivalent mixing depths of CH_3I (see section 3.1). All photolysis rate coefficients were adjusted using an adjustment factor (labeled here "cloud correction factor (CCF)") considering actual solar/cloud conditions. For the purpose of removing the case of the significant cloud effect on actinic flux, the flights with CCF$<$0.75 were excluded. After filtering, 47 acceptable events led to 10 independent flux determinations. The reduction in the number of independent flux estimation reflects the fact that typically 4 or more BL runs from a given flight were used in making one independent flux determination.

3. APPROACH AND MODEL DESCRIPTION

3. 1 Approach

The method for the evaluation of the CH_3I flux (F_{CH_3I}) in this work is based on the mass balance photochemical model (MBPCM) approach, which is similar to that described by Shon *et al.* (2001). All forms of the MBPCM approach for determining the CH_3I flux require that the regions under investigation have reasonably high levels of CH_3I horizontal

Table 1. Summary of model input conditions.

Flight No.	Sampling time (local)	Lat. (−: S)	Long. (−: W)	T^a (°C)	$*Td^a$ (°C)	$[O_3]^a$ (ppbv)	$[CO]^a$ (ppbv)	$^+[NO]^a$ (pptv)	$[NO_x]^b$ (pptv)	BL h (km)	EMD (km)
5	10:12	17.7	−158.2	25.7	19.1	32.2	87.7	8.7	32.3	0.6	2.5
6	12:33	2.5	−155.0	23.0	18.1	25.4	78.9	6.7	23.6	1.0	1.8
16	12:54	−54.1	159.2	2.2	−3.1	21.4	68.5	2.5	5.8	0.4	2.5
18	05:58	−45.0	144.5	9.5	4.8	21.0	69.2	3.9	15.2	1.0	1.6
21	04:34	−42.5	142.1	9.5	1.1	20.7	66.4	2.9	6.9	0.9	2.1
22	15:45	−41.4	139.3	10.5	1.6	18.4	64.8	2.0	4.7	1.0	1.4
24	10:15	−45.2	143.6	10.0	5.8	20.8	63.6	2.6	6.1	0.5	1.5
29	11:44	−32.7	159.2	20.1	11.0	21.4	61.2	4.4	12.4	0.7	1.6
31	16:20	1.9	−156.4	22.5	18.1	9.8	68.8	2.6	6.2	0.5	1.9
32	10:39	2.7	−156.2	22.7	18.8	13.3	70.0	5.5	13.2	0.5	1.1

(a) Median observations; (b) Model calculated quantity; (*) Dew Point; (+) For detailed discussion on [NO], see the text.

homogeneity. Given the assumption that the BL is well mixed, in its final form the mass balance equation is shown in an Eq. (2) :

$$\frac{d[CH_3I]}{dt}=\frac{F_{CH_3I}}{EMD}-(J_{CH_3I}+k[OH])[CH_3I]+\frac{1}{EMD}\int_{hBL}^{hBuL} w\left[\frac{\partial[CH_3I(z)]}{\partial z}\right]dz \qquad (2)$$

hBL

where, the equivalent mixing depth (EMD) defines the CH_3I equivalent mixing depth which can best be represented by Eq. (3) :

$$EMD=\frac{\int[CH_3I(z)]dz}{[CH_3I]_{BL}} \qquad (3)$$

In the Eq. (3), $[CH_3I]_{BL}$ represents the average CH_3I concentration in the MBL. Fig. 2 shows a schematic representation of the EMD evaluated for Flight 32. The remaining terms in Eq. (2) include J_{CH_3I}, a photolysis rate coefficient; k_{OH}, the reaction rate coefficient for reaction with OH; "w," the mean vertical velocity; and $\partial[CH_3I(z)]/\partial z$, the vertical gradient of CH_3I within the BuL.

The first term on the right-hand side of Eq. (2) relates to the CH_3I sea-to-air flux; the second term defines the loss of CH_3I due to photolysis and oxidation by OH; and the third term evaluates the effects of large scale mean vertical motion on the levels of CH_3I. The latter term presents much the same problem as that cited for EMD in that it obviously varies some with time, but the absence of continuous readings of the CH_3I gradient between the BL and BuL makes it impractical to evaluate this variability. In addition, only 24 hr average values were available for "w" from NCEP meteorological data. Thus, the approach taken here was similar to that used for the EMD evaluation; we assumed that, to a first approximation, its value was non-time dependent. From a practical point of view, the "best estimate" for F_{CH_3I} can be assessed by chis-quared testing. Fig. 3 shows the result of this procedure for Flight 24. Meanwhile, CH_3I destruction rates through photolysis in the tropical MBL were $>90\%$ of the total destruction rate, while those through OH oxidation were $<10\%$. CH_3I loss via OH oxidation was insignificant in the tropical MBL as well as over the Southern Ocean.

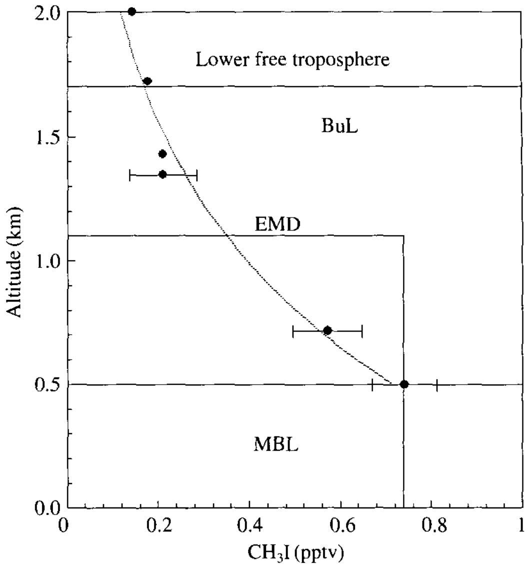

Fig. 2. Evaluation of the CH_3I equivalent mixing depth (EMD) for flight 32. The straight line at 1.1 km is the EMD for flight 32. The closed circles with horizontal bars represent the observed averages for CH_3I for horizontal flight legs at 0.5, 0.7, and 1.3 km. The horizontal bars are the 1 sigma values on CH_3I. The dotted line defines the best curve fit to the observed CH_3I mixing ratios based on the six altitudes.

3. 2 Model description

The MBPCM was coupled to a full $HO_x/NO_x/CH_4$/NMHC time-dependent photochemical box model constrained by measured values of NO, CO, O_3, H_2O, H_2O_2, CH_3OOH, and UV irradiance. When significant BL OH observations were available at the time of the CH_3I observations, these were typically used to further constrain the model generated OH profiles by adjusting critical J values. The critical parameter for the evaluation of the CH_3I flux-J value for CH_3I-was derived from the absorption cross-section and quantum yield reported by Rattigan *et al.* (1997). The current MBPCM approach has been previously used to assess both DMS sea-to-air fluxes as well as the oxidation products

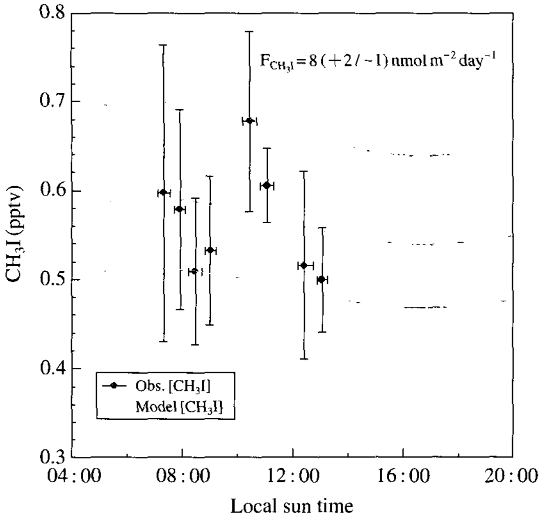

Fig. 3. Evaluation of the CH_3I flux for flight 24 using the MBPCM approach. Three solid lines are the diel CH_3I profiles generated from the model based on averaged CH_3I observations as given by the solid circles. The best fit to the data gives a CH_3I flux of 8 nmol m^{-2} day^{-1}. The solid line above the best fit and that the below the best fit represent the upper limit (10) and lower limit (7) values of the model estimated CH_3I fluxes, respectively. Horizontal bars on each CH_3I data point define the time period over which the average value was calculated. Vertical bars define the 1 sigma value for the CH_3I observations averaged over a given horizontal leg.

from DMS (Shon *et al.*, 2001 and references therein). Details concerning the photochemical box model have been previously described by Davis *et al.* (1996).

Table 2. Sea-to-Air CH_3I Flux Estimates.

Flight Number	Date (1995)	Latitude (− : S)	Longitude (− : W)	Flux (nmol m^{-2} day^{-1})
5	11/06	17.7	−158.2	33
6	11/08	2.5	−155.0	12
16	11/27	−54.1	159.2	5
18	12/01	−45.0	144.5	10
21	12/04	−42.5	142.1	8
22	12/05	−41.4	139.3	4
24	12/08	−45.2	143.6	8
29	12/16	−32.7	159.2	9
31	12/19	1.9	−156.4	12
32	12/20	2.7	−156.2	10

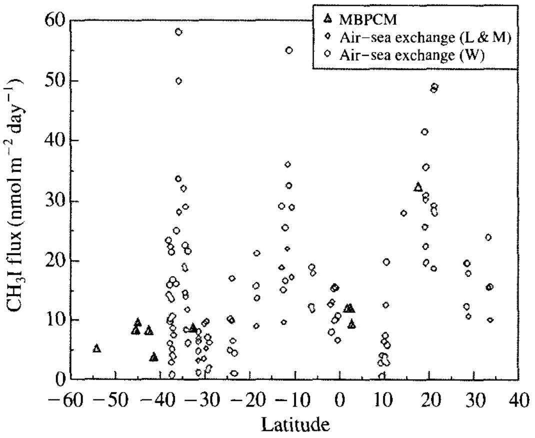

Fig. 4. Latitudinal distributions of CH_3I fluxes during the ACE 1 field program. Triangle symbols are fluxes estimated by the MBPCM; solid circles are those calculated as the product of the transfer velocity of Wanninkhof (1992) and the surface seawater concentration measured by Moore and Groszko (1999); open circles are those calculated as the product of the transfer velocity of Liss and Merlivat (1986) and the surface seawater concentration.

4. RESULTS AND DISCUSSION

4.1 CH_3I flux

CH_3I fluxes estimated using airborne observations are shown in Table 2 and Fig. 4, ranging from 4 to 33 nmol m^{-2} day^{-1}. The average value from this ensemble was 11 ± 8 nmol m^{-2} day^{-1}. Fig. 4 shows the same data as given in Table 2, but here the fluxes are plotted as a function of latitude. In the Southern Ocean CH_3I fluxes were relatively lower than those in the tropical regions. In the Southern Ocean CH_3I fluxes ranged from 4 to 10 nmol m^{-2} day^{-1} with an average value of 7 ± 2. In contrast, the fluxes in the tropical regions ranged from 10 to 33 nmol m^{-2} day^{-1} with an average value of 17 ± 11. CH_3I fluxes in the tropical regions were higher by a factor of 2 than those in the Southern Ocean. From these data one sees a trend of a decreasing CH_3I flux with increasing southerly latitude. The calculated flux might be driven in part by the change in photolysis frequency. The CH_3I fluxes derived from shipboard measurements are discussed in section 4.2. The shipboard atmospheric CH_3I concentrations are in the range of 0.1 to 1.7 pptv with an average value of 0.7 ± 0.3, similar to the measurements from the *C-130*.

It should be noted that large variation in the fluxes results from the combination of the temporal and spatial variability of wind speed and seawater CH_3I concentrations. An average wind speed during seawater CH_3I observation period was 6.3 ± 2.2 m s^{-1}. Seawater CH_3I concentrations for the ACE 1 ranged from 2.5 to 16.1 pmol L^{-1} with an average value of 4.8 ± 1.9. Seawater CH_3I concentration in the extratropical regions were significantly higher than those in the tropical regions by a factor of 1.5-1.7. Detailed discussion on seawater CH_3I distribution for ACE 1 was described in Moore and Groszko (1999). They attributed the tendency for variability in seawater CH_3I concentrations to water temperature and irradiance, and on a smaller space scale, they also found the indication of a correlation between methyl iodide with chlorophyll *a*. It has been reported that seawater levels of CH_3I are likely to be correlated with ocean biological productivity (Bassford *et al.*, 1999). Bassford *et al.* (1999) found that concurrent observations of CH_3I and dimetyl sulfide (DMS) in marine air showed a clear association. This was supported by a statistical analysis indicating a very significant degree of covariance, implying common open-ocean source regions. In contrast, different spatial and temporal patterns for each of the gases were observed. For instance, Baker *et al.* (2000) showed that distinct sources dominate their production (i.e., specific species of phytoplankton for DMS and macroalgae for CH_3I). It has been suggested that photochemical production may be a significant source of CH_3I within the open ocean (Moore and Zafiriou, 1994). At this moment the source mechanism of methyl iodide in seawater is still uncertain.

Assuming that CH_3I is related to biological activity in seawater, one approach taken in the ACE 1 to further categorize the Southern Ocean CH_3I flux has involved relating the estimated flux to other ocean characteristics such as the type of surface water mass. For example, during the ACE 1 three different surface water masses were identified during the "intensive" campaign (Bates *et al.*, 1998). These differed substantially in salinity as well as in biological activity. These have been labeled subtropical convergence zone (STCZ, <43° S), subantarctic water zone (SAZ, 43°-49° S), and Antarctic zone (AZ, >49° S). The STCZ had the highest salinity value at >34.8 psu, while the AZ had the lowest value at <34.2 psu.

During the "intensive" period of the ACE 1, two flux determinations were made in the STCZ, two in the SAZ, and one in the AZ. The STCZ data were recorded on Flights 21 and 22. As shown in Fig. 4 the values of these two flux estimates varied by about a factor of 2, ranging from 4 to 8 nmol m^{-2} day^{-1}. The flux values estimated for the SAZ (e.g., 8-10 nmol m^{-2} day^{-1}) were somewhat higher than those for the STCZ based on analysis of Flights 18 and 24. In the third and final zone (AZ) the CH_3I flux (e.g., 5 nmol m^{-2} day^{-1}) was similar to those in the STCZ and was significantly lower than those in the SAZ based on analysis of Flight 16. For one transit flight of the ACE 1 field experiment (e.g., Flight 29), the CH_3I flux value of 9 nmol m^{-2} day^{-1} was similar to the flux values in the SAZ. The daily average wind speed (obtained from NCEP meteorological data) appears fairly constant over the time period of the measurements. Thus, a likely cause for the large variability in the CH_3I flux field is the inhomogeneity in seawater CH_3I levels because significant temporal and spatial variations in seawater CH_3I were observed.

The CH_3I fluxes in the tropical regions were significantly higher than those in the Southern Ocean, ranging from 10 to 33 nmol m^{-2} day^{-1} and give an average value of 17 ± 11. These results were based on Flights 5, 6, 31, and 32. Fluxes for Flights 6, 31, and 32 showed fairly uniform. In contrast, the CH_3I flux for Flight 5 showed significantly higher values by a factor of 3, compared to the three other flights. This higher flux for Flight 5 is consistent with the flux derived from seawater CH_3I concentrations at the same location (see Fig. 4). Section 4.2 contains a detailed discussion on the fluxes derived from seawater measurements. These tropical regions are more productive zones so that biological activities are higher than in oligotropic open ocean. These results however do not imply that CH_3I fluxes are solely associated with biological activities in seawater since irradiance and water temperature are also high in tropical regions.

During the ACE 1 field experiment, atmospheric CH_3I levels were somewhat lower than those reported in the literature. The average atmospheric CH_3I concentration in the MBL (< 1 km) in the tropical region (15° S-15° N) was 0.6 ± 0.1 pptv (a median value of 0.58 pptv), while that over the Southern Ocean (> 40° S) was 0.48 ± 0.22 pptv (a median value of 0.43). There were no strong spatial trends in MBL mixing ratios of methyl iodide over the Southern Ocean and the significant temporal increase in average mixing ratios between late Nov. and early Dec. was attributed to a rapid transition to summer conditions in the regions (Blake *et al.*, 1999). Compared to CH_3I levels at the northern Pacific (Li *et al.*, 1999) and at a northern Atlantic coastal site (Bassford *et al.*, 1999), those in the tropical regions during the ACE 1 field experiment were lower by a factor of 2-6, while atmospheric CH_3I levels over the Southern Ocean during ACE 1 were lower by a factor of 5 than those in the Antarctic atmosphere (Reifenhäuser and Heumann, 1992).

In spite of the weak statistical base it is somewhat reassuring to find that the current CH_3I flux results obtained using the MBPCM are not systematically different from those previously reported in the literature based on the air-sea exchange model. For instance, local CH_3I flux from this study is in the value range reported in the literature and it is close to the value (e.g., 9.3 nmol $m^{-2} day^{-1}$) in the southern North Sea reported by Campos *et al.* (1996). In contrast, the local CH_3I flux in the south polar sea was significantly higher and reported to be 42.3 nmol $m^{-2} day^{-1}$ by Reifenhauser and Heumann (1992). In the eastern Pacific Ocean (40° N-32° S) a slightly higher flux of 27 nmol $m^{-2} day^{-1}$ was reported by Singh *et al.* (1983).

4. 2 Comparison of the MBPCM with the air-sea exchange model

Direct in-situ intercomparison of CH_3I flux using the air-sea exchange model with that using the MBPCM was not available in time and space. However, similar location and close time period for sampling allow us to compare these two methods. Methyl iodide concentration in seawater was highly supersaturated (i.e., average saturation anomaly of about 4500%) so that the CH_3I flux using the air-sea exchange model was calculated as the product of the seawater CH_3I concentration and the exchange coefficient (V_p). The latter is calculated using Liss and Merlivat (1986) parameterization. For the exchange coefficient, methyl iodide's Schmidt number was estimated from that for methyl bromide (De Bruyn and Saltzman, 1997) with assumption that the ratio of the diffusivities is inversely proportional to the ratio of the molar volumes to the power of 0.6 (Wilke and Chang, 1955). For the CH_3I flux estimation, Wanninkhof (1992) parameterization was also used for the upper limit values.

The fluxes estimated from the air-sea exchange model are also shown in Fig. 4. Those using Liss and Merlivat (1986) (hereafter identified as L & M) ranged from 0.5 to 33.6 nmol $m^{-2} day^{-1}$ and the average value was 11.4. CH_3I fluxes using L & M parameterization showed higher values in tropical regions and northern extratropical regions than in the southern extratropical regions by the factor of 1.6. The fluxes using Wanninkhof (1992) (hereafter identified as W (92)) were doubled. Although direct flux intercomparison in terms of time and space was not available during the ACE field program, relative comparison of CH_3I fluxes was possible. The sampling time period for seawater CH_3I observations was mid-Oct. through early Nov., while that for airborne CH_3I observations was early Nov. through late Dec. Time overlap is only one day, but the locations are not overlapped. For the entire ACE 1 sampling locations, average CH_3I flux (e.g., -11 nmol $m^{-2} day^{-1}$) estimated from the air-sea exchange model was consistent with that from the MBPCM. In general, fluxes for the air-sea exchange model bracket those for the MBPCM. In the latitudinal range of 30° −40° S the average flux for L & M was 9.9 ± 8.7 nmol m^{-2} day^{-1} and the MBPCM flux for the similar location (Flight 29) was 9 nmol m^{-2} day^{-1}. In the sub-tropical regions (10° S-10° N) average flux for L & M was 7.7 ± 4.1 nmol m^{-2} day^{-1}, whereas that for the MBPCM (i.e., Flights 6, 31, and 32) was similar to W (92) (i.e., 11 nmol m^{-2} day^{-1}). The CH_3I flux for Flight 5 in the northern tropical regions was also closer to W (92) than L & M. The fluxes in the STCZ for the MBPCM were closer to L & M than W (92) in adjacent regions. In spite of the weak statistical base it is somewhat reassuring to find that our results (MBPCM) are generally consistent with those previously reported (air-sea exchange model) by Moore and Groszko (1999). At this time we believe it would be premature to draw any final conclusion of selecting one method over the other with respect to L & M and W (92). This results from the fact that the number of detailed comparisons was small and that the conditions under which the comparisons were made were far from ideal. In addition, our results are less uncertain compared to the air-sea exchange model (flux uncertainty of a factor of 2). Section 4.3 contains a detailed discussion on uncertainty in flux determination.

4. 3 Sensitivity and uncertainty analyses of CH_3I flux

To explore the potential magnitude of systematic errors in the CH_3I flux estimates, model sensitivity calculations were carried out for each major variable in Eq (1) (i.e., EMD, $[CH_3I]_{(obs)}$, J, [OH], and $\int w (\partial CH_3I/\partial z) dz$). The procedure followed involved increasing and then decreasing the value of each variable by a factor of 2 and then examining the effect on the calculated flux. Thus, the sensitivity of the flux estimate to possible systematic errors in each variable was defined in terms of the corresponding change in the value of F_{CH_3I}. Table 3 summarizes the results from this analysis by displaying the average values resulting from following this procedure for all 10 flux estimates. Not surprisingly, it can be seen that the CH_3I flux is found to be linearly dependent on the EMD, $[CH_3I]_{(obs)}$, and J_{CH_3I}. It is somewhat less linear for $\int w (\partial CH_3I/\partial z) dz$. However, it is almost nonlinearly dependent on [OH]. On average, the contribution of large-scale mean vertical motion to the CH_3I flux was 30%. The lack of sensitivity of the flux estimates toward [OH] reflects the insignificance of this term as loss process for CH_3I (e.g., less than 10%) relative to the loss from photolysis.

Table 3. Summary of sensitivity test of MBPCM to CH_3I flux.

Input parameters	Change factor	Change factor in $F_{sea-air}$
EMD	±2	±2
$[CH_3I]_{obs}$	±2	±2
J	±2	±2
[OH]	±2	±1.1
$\int_{hBL}^{hBuL} \left[w \frac{\partial [CH_3I(z)]}{\partial z} \right] dz$	±2	±1.5

The magnitude of the random error associated with each CH_3I flux determination was estimated from an error propagation analysis. The resulting values ranged from 30 to 50%, with an average of 40%. The three major contributors to this overall error were: J_{CH_3I}, $CH_3I_{(obs)}$, and EMD (i.e., 30, 15, and 20%, respectively). The error associated with J_{CH_3I} was related to the uncertainty in the absorption cross-section area and the parameterized actinic flux. The error on the cross-section area was typically 5% (Rattigan *et al.*, 1997). The uncertainty specified for the value of $CH_3I_{(obs)}$ primarily reflects atmospheric fluctuations of this species rather than any inherent instrument precision problems in measuring CH_3I. Regarding the final parameter, EMD, both the uncertainty in defining the BL height as well as an in accurately assessing the vertical gradient in CH_3I contributed equally to the overall error. The error associated with the major contributor, J value, was primarily related to the uncertainty in the estimation of the CCF as well as the actinic flux. This reflects the fact that clouds were often encountered during the ACE 1 airborne sampling program.

5. CONCLUSION

The MBPCM approach was used to evaluate sea-to-air CH_3I fluxes in the Pacific Ocean and the Southern Ocean. These evaluations were based on 10 airborne observations of the ACE 1 field study in Nov. and Dec. of 1995. Eleven BL sampling events covered the latitude range of 2° N to 55° S and encompassed a flux range of 4 to 33 nmol m^{-2} day^{-1}. The average value emerging was 11 ± 8 nmol m^{-2} day^{-1}. The CH_3I fluxes in the tropical regions were significantly higher than those in the Southern Ocean, ranging from 10 to 33 nmol m^{-2} day^{-1} and gave an average value of 17 ± 11. During the ACE 1 field experiment, atmospheric CH_3I levels were somewhat lower than those reported in the literature. The average atmospheric CH_3I concentration in the MBL (< 1 km) in the tropical regions was 0.7 ± 0.2 pptv, while that in the Southern Ocean was 0.5 ± 0.2 pptv. When compared to the MBPCM, methyl iodide fluxes estimated by the air-sea exchange model (L & M) ranged from 0.5 to 33.6 nmol m^{-2} day^{-1} and the average value was 11.4. In spite of the weak statistical base it is somewhat reassuring to find that the current CH_3I flux results obtained using the MBPCM are not systematically different from those previously reported in the literature based on the air-sea exchange model.

ACKNOWLEDGMENTS

This work was supported by the Climate Environment System Research Center sponsored by the SRC program of Korea Science and Engineering. The author wishes to thank Dr. D. Blake from University of California at Irvine, USA for providing airborne CH_3I data set. The author also wishes to thank Dr. R. Moore from Dalhousie University, Canada for providing seawater CH_3I data set.

REFERENCES

Allan, B.J., G. McFiggans, J.M.C. Plane, and H. Coe (2000) Observations of iodine monoxide in the remote marine boundary layer. J. Geophys. Res., 105, 14363-14369.

Andreae, M.O. (1986) The ocean as a source of atmospheric sulfur compounds. In The Role of Air Sea Exchange in Geochemical Cycling, ed. P. Buat-Menard, D. Reidel, Netherlands, 331-362.

Baker, A.R., S.M. Turner, W.J. Broadgate, A. Thompson, G.B. McFiggans, O. Vesperini, P.D. Nightingale, P.S. Liss, and T.D. Jickells (2000) Distribution and sea-air fluxes of biogenic trace gases in the eastern Atlantic Ocean. Global Biogeochemical Cycles, 14, 871-886.

Bassford, M.R., G. Mickelss, P.G. Simmonds, A.C. Lewis, M.J. Pilling, and M.J. Evans (1999) The concurrent observation of methyl iodide and dimethyl sulphide in marine air; implications for sources of atmospheric methyl iodide. Atmos. Environ., 33, 2373-2383.

Bates, T.S., V.N. Kapustin, P.K. Quinn, D.S. Covert, D.J. Coffman, C. Mari, P.A. Durkee, W.J. De Bruyn, and E.S. Saltzman (1998) Processes controlling the distribution of aerosol particles in the lower marine boundary layer during the First Aerosol Characterization Experiment (ACE 1). J. Geophys. Res., 103, 16369-16383.

Blake, N.J., C.H. Kang, D.C. Thornton, A.R. Bandy, E. Atlas, F. Flocke, J.M. Harris, F.S. Rowland, D.R. Blake, O.W. Wingenter, and B.C. Sive (1999) Aircraft measurements of the latitudinal, vertical, and seasonal variations of NMHCs, methyl nitrate, methyl halides, and DMS during the First Aerosol Characterization Experiment (ACE 1). J. Geophys. Res., 104, 21803-21817.

Campos, M.L., P.D. Nightingale, and T.D. Jickells (1996) A comparison of methyl iodide emissions from seawater and wet depositional fluxes of iodine over the southern North Sea. Tellus, 48B, 106-114.

De Bruyn, W.J. and E.S. Saltzman (1997) Diffusivity of methyl bromide in water. Mar. Chem., 56, 51-57.

Itoh, N., M. Tsujita, T. Ando, G. Hisatomi, and T. Higashi (1997) Formation and emission of monohalomethanes from marine algae. Phytochemistry, 45, 67-73.

Li, H.-J., Y. Yokouchi, and H. Akimoto (1999) Measurement of methyl halides in the marine atmosphere. Atmos. Environ., 33, 1881-1887.

Liss, P.S. and Slater (1974) Flux of gases across the air-sea interface. Nature, 247, 181-184.

Liss, P.S. and L. Merlivat (1986) Air-sea gas exchange rates: Introduction and synthesis, in The Role of Air-Sea Exchange in Geochemical Cycling. Edited by P. Buat-Mnard, pp. 113-127, D. Reidel, Norwell, Mass.

Lovelock, J.E., R.J. Maggs, and R.J. Wade (1973) Halogenated hydrocarbons in and over the Atlantic. Nature, 256, 193-194.

Manley, S.L. and M.N. Dastoor (1988) Methyl iodide production by kelp and associated microbes. Mar. Bio., 98, 477-482.

Moore, R.M. and O. Zafiriou (1994) Photochemical production of methyl iodide in seawater. J. Geophys. Res., 99, 16415-16420.

Moore, R.M. and W. Groszko (1999) Methyl iodide distribution in the ocean and fluxes to the atmosphere. J. Geophys. Res., 104, 11163-11171.

Rattigan, O.V., D.E. Shallcross, and R.A. Cox (1997) UV absorption cross-sections and atmospheric photolysis rates of CF_3I, CH_3I, C_2H_5I, and CH_2ICl. Journal of Chemical Society Faraday Transaction, 93, 2839-2846.

Reifenhäuser, W. and K.G. Heumann (1992) Determinations of methyl iodide in the Antarctic atmosphere and the south polar sea. Atmos. Environ., 26, 2905-2912.

Shon, Z.-H. (1999) Photochemical assessment of oceanic emissions of DMS and its oxidation to SO_2 based on airborne field observations, Ph. D. dissertation, Georgia Institute of Technology, Atlanta, GA, USA.

Shon, Z.-H., D. Davis, G. Chen, G. Grodzinsky, A. Bandy, D. Thornton, S. Sandholm, J. Bradshaw, R. Stickel, W. Chameides, G. Kok, L. Russell, L. Mauldin, D. Tanner, and F. Eisele (2001) Evaluation of the DMS flux and its conversion to SO_2 over the Southern Ocean. Atmos. Environ., 35, 159-172.

Shon, Z.-H. and N. Kim (2002) A modeling study of halogen chemistry's role in marine boundary layer ozone. Atmos. Environ., 36, 4289-1298.

Singh, H.B., L.J. Salas, and R. Stiles (1983) Methyl halides in and over the eastern Pacific (40N-32S), J. Geophys. Res., 88, 3684-3690.

Smethie, W.M., Jr., T. Takahashi, D.W. Chipman, and J.R. Ledwell (1985) Gas exchange and CO_2 flux in the tropical Atlantic Ocean determined from ^{222}Rn and pCO_2 measurements. J. Geophys. Res., 90, 7005-7022.

Wanninkhof, R. (1992) Relationship between wind speed and gas exchange over the ocean. J. Geophys. Res., 97, 7373-7382.

Wilke, C.R. and P. Chang (1955) Correlation of diffusion coefficients in dilute solutions. Am. Inst. Chem. Eng. J. 1, 265-270.